Electronic Supplementary Material (ESI) for RSC Advances.

Supplementary files

Nitrogen-doped lignin-derived carbon for catalytic reduction of hexavalent chromium via HCOOH-mediated hydrogenation

Yun Liu*, Haihua Yang

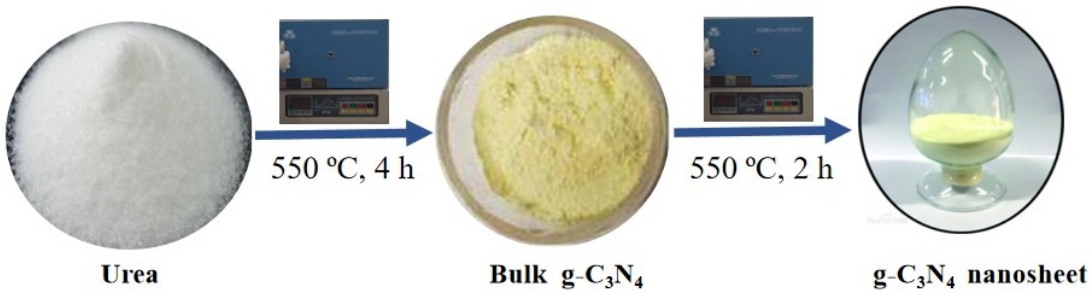

Fig. S1 Preparation of g-C_3N_4 nanosheets through duplicate thermal decomposition of urea.

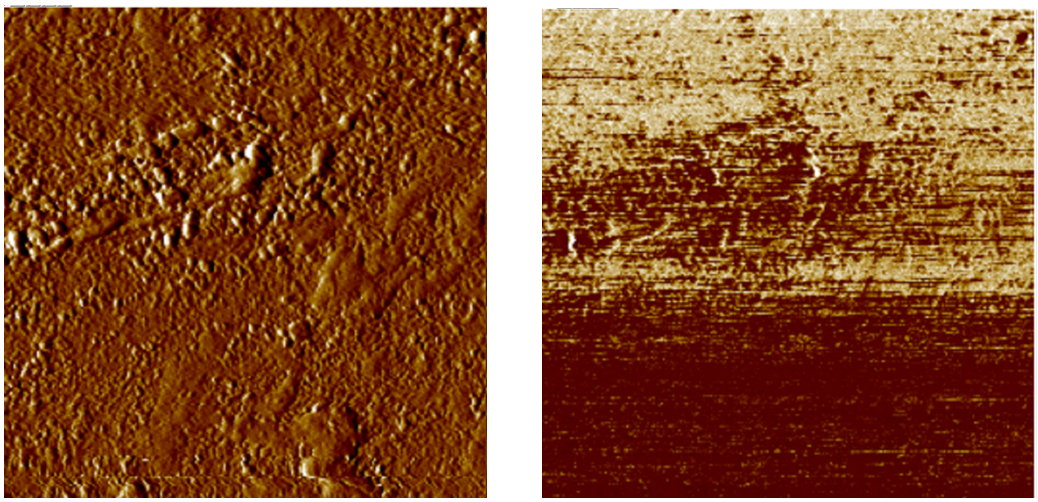

Fig. S2 AFM images of N@C-g-C_3N_4. left picture is for amplitude, and right picture stands for phase image.

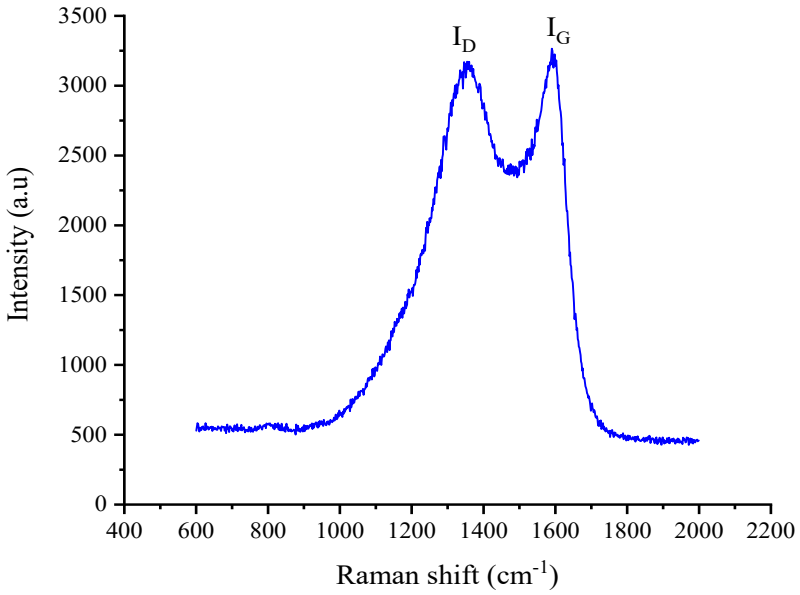

Fig. S3 Raman spectrum of N@C-g-C_3N_4-950. The peak at 1350 is assigned to disordered sp3 carbon (I_D) and the peak at 1590 nm is assigned to graphitic sp^2 carbon (I_G).

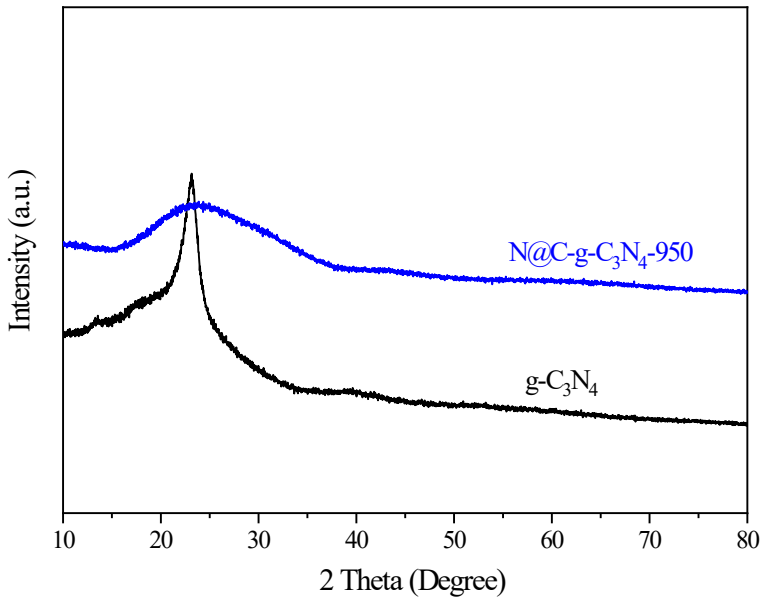

Fig. S4 shows XRD pattern of N@C-g-C_3N_4-950 and g-C_3N_4 template.

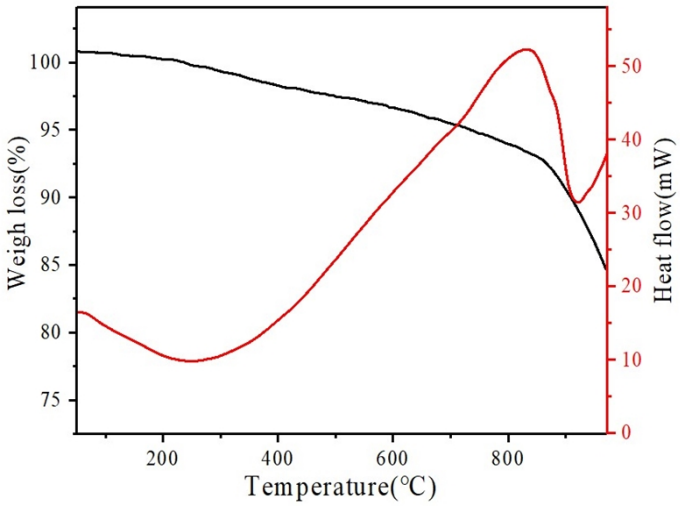

Fig. S5 TGA/DSC analysis of N@C-g- C_3N_4-950.

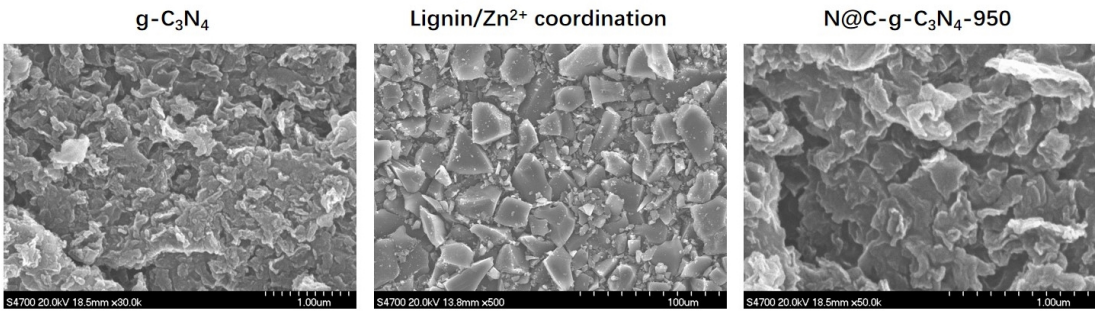

Fig. S6 SEM morphology of g-C_3N_4 , lignin/Zn^{2+} coordination (LC carbon) and N@C-g-C_3N_4-950.

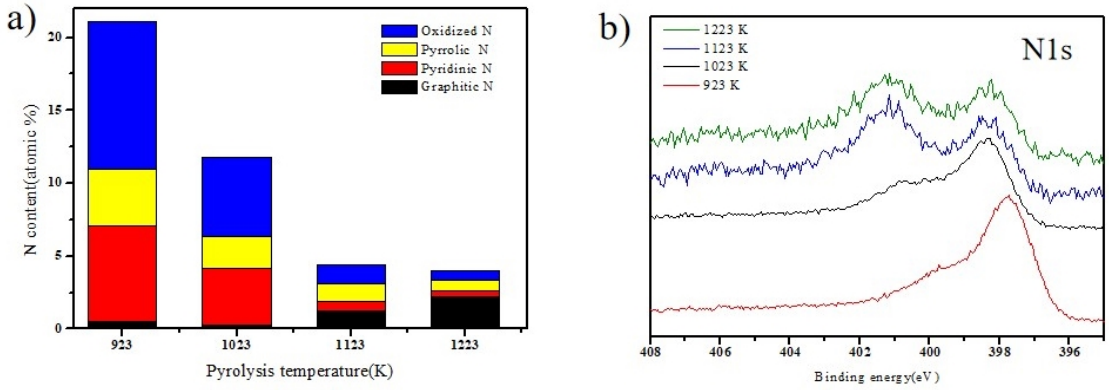

Fig, S7 The relative contents of nitrogen species in N@C with different annealing temperatures of 923 K, 1023 K, 1123 K, and 1223 K.

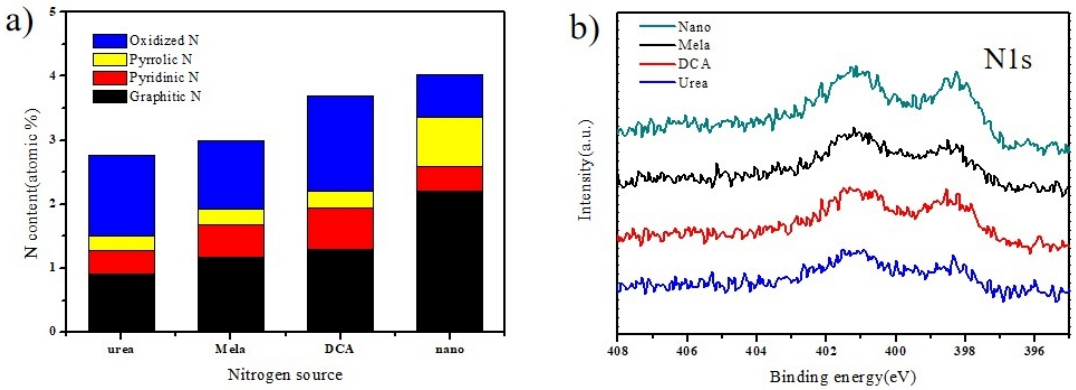

Fig.S8 The relative contents of nitrogen species in N@C with different nitrogen dopants of urea, mela, DCA and g-C_3N_4.

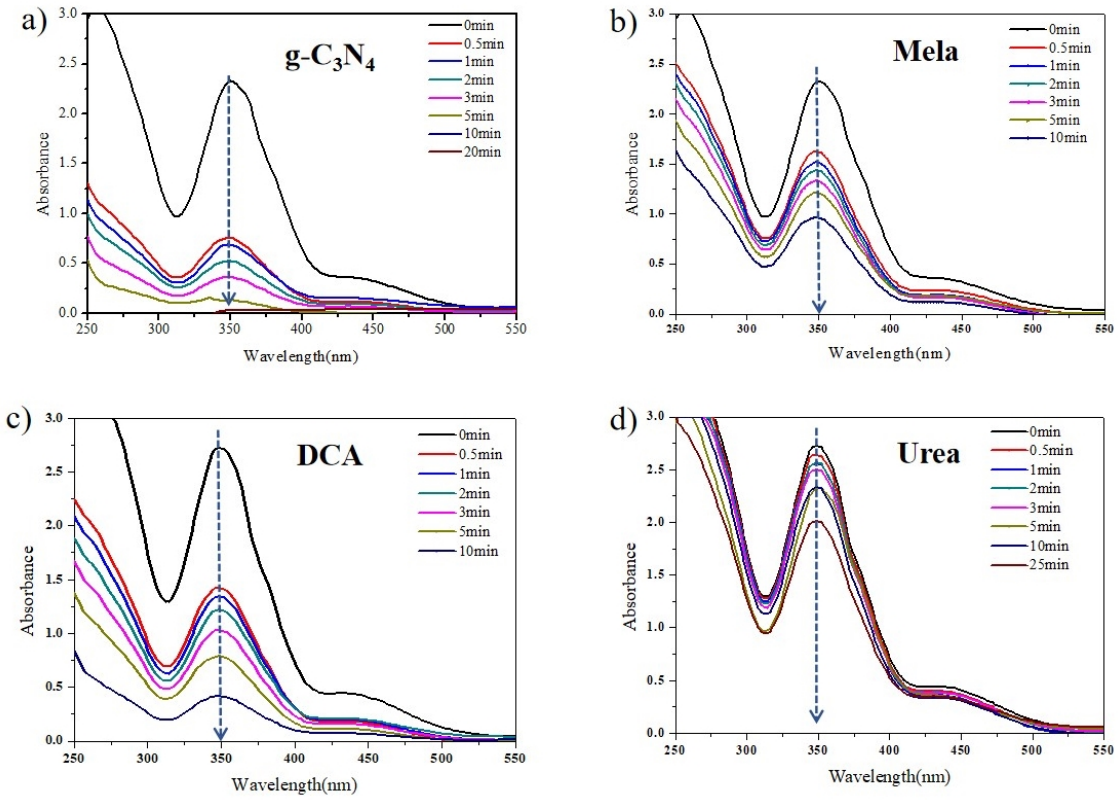

Fig. S9 Cr^{6+} reduction catalyzed by N@C with different nitrogen dopant. Reaction conditions: 25 mL $K_2Cr_2O_7$ (0.68 mM) , 1 mL HCOOH (98%), 25 mg catalyst, temperature 50 °C, stirring rate 500 rpm.

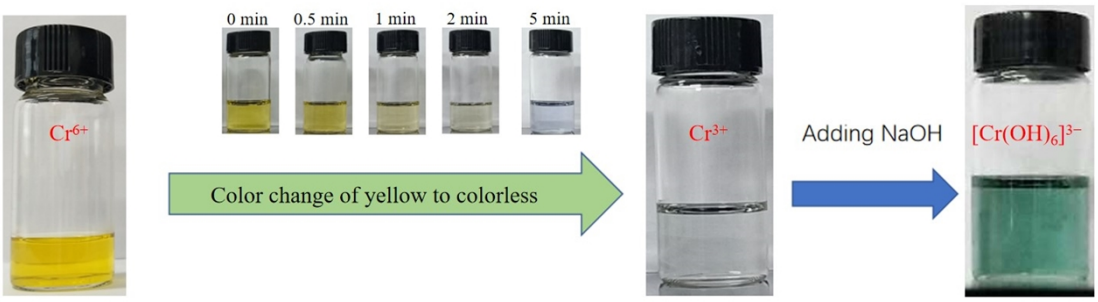

Fig. S10 The photographs of Cr^{6+} reduction conversion into colorless Cr^{3+} by N@C-g-C_3N_4-950 in the presence of HCOOH at different time intervals; and the photograph of green solution of hexahydroxochromate (III) obtained after the addition of excess NaOH solution.

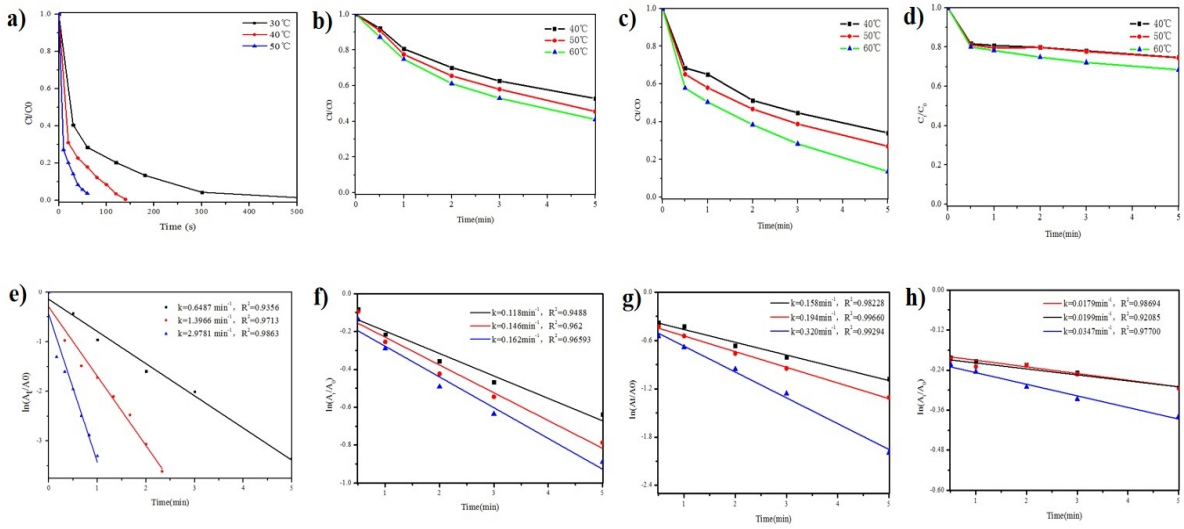

Fig. S11 Apparant rate constant (k) of the catalytic reduction of Cr^{6+} with N@C catalysts. (a,e) g-C_3N_4; (b,f) Mela; (c, g) DCA; (d, h) Urea. Reaction conditions: 25 mL $K_2Cr_2O_7$ (0.68 mM) , 1 mL HCOOH (98%), 25 mg catalyst, stirring rate 500 rpm.

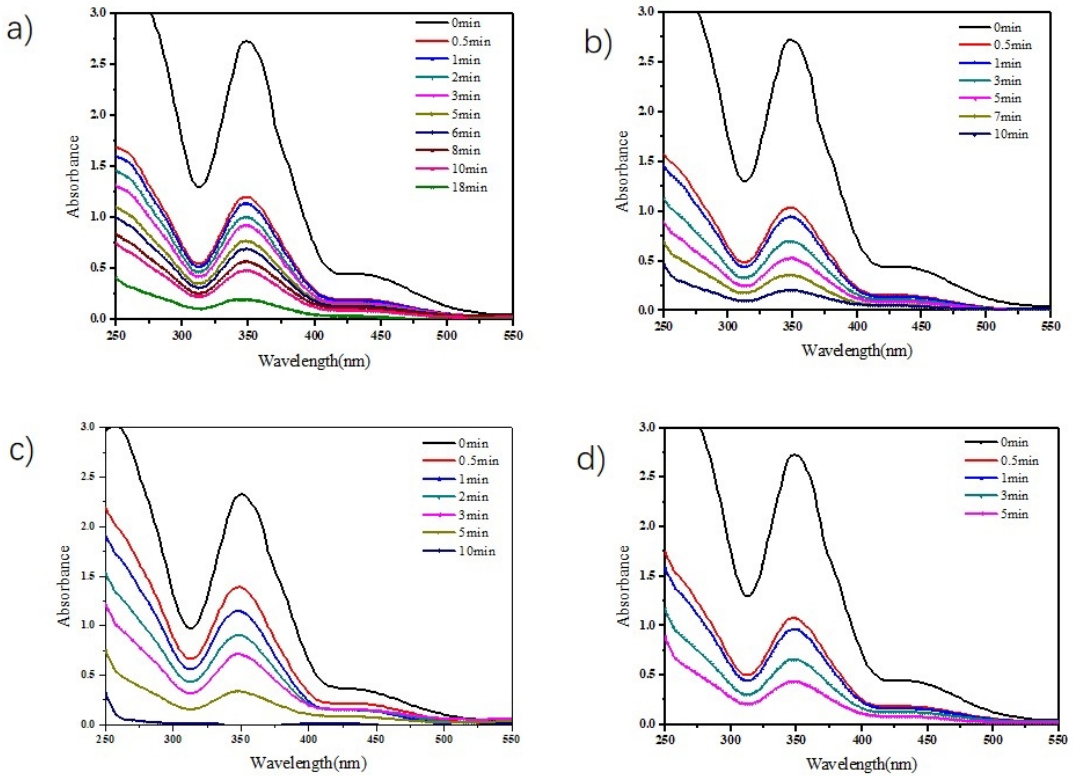

Fig. S12 Effect of HCOOH concentration on Cr^{6+} reduction by N@C-gC_3N_4-950. (a) 0.01 mM; (b) 0.02 mM; (c) 0.03 mM; (d) 0.04 mM. Other reaction conditions: 25 mL $K_2Cr_2O_7$ (0.68 mM) , 25 mg catalyst, temperature 50°C, stirring rate 500 rpm.

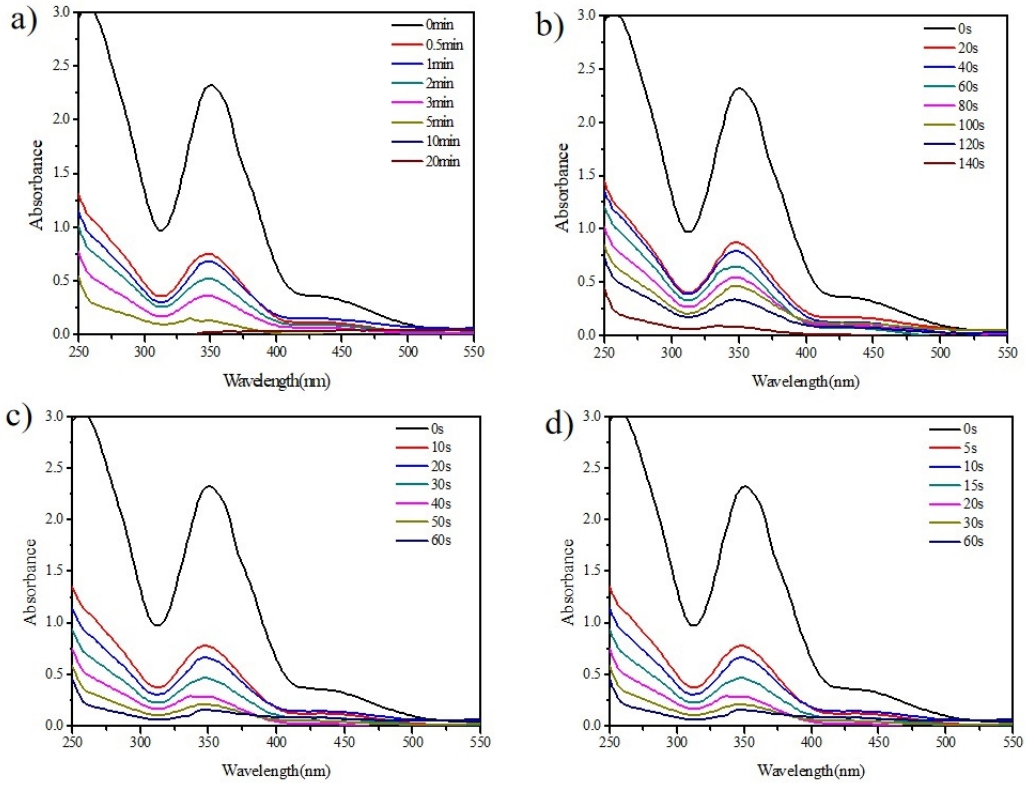

Fig. S13 Effect of reaction temperature on Cr^{6+} reduction in the presence of HCOOH and N@C-gC3N4. (a) room temperature (RT); (b) 40 ºC; (c) 50 ºC; (d) 60 ºC. Other reaction conditions: 25 mL $K_2Cr_2O_7$ (0.68 mM) , 1 mL HCOOH (98%), 25 mg catalyst, stirring rate 500 rpm.

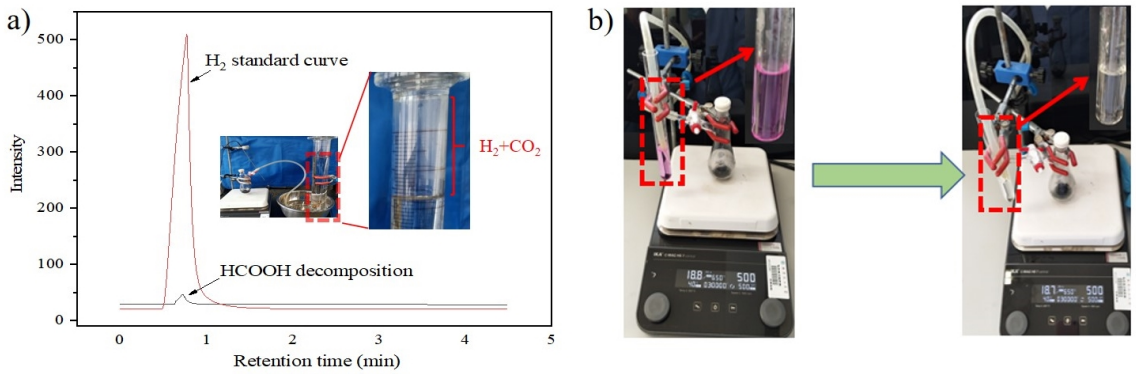

Figure S14 (a) Determination of H_2 decomposited from HCOOH by GC detection; (b) CO_2 evolution from HCOOH was monitored by phenolphthale in coloration method. Reaction conditions: 25 mL $K_2Cr_2O_7$ (0.68 mM) , 1 mL HCOOH (98%), 25 mg catalyst, temperature 30 °C, stirring rate 500 rpm.

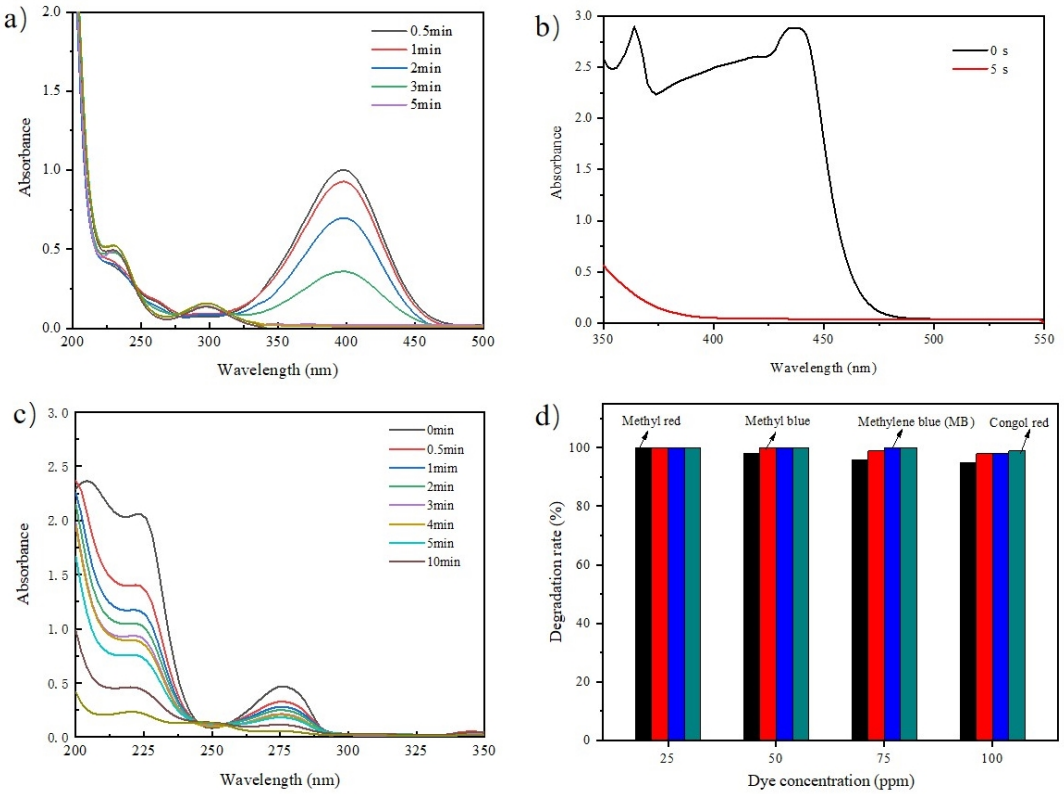

Fig. 15 Extended hydrogenation reactions and removal of organic dyes by N@C-g-C_3N_4. (a) 4-NP; (b) $K_3[Fe(CN)_6]$; (c) BPA; (d) organic dyes. Reaction conditions: 25 mg catalyst, room temperature, stirring rate 500 rpm.

Table S1 The atomic ratio (calculation from XPS analysis) and BET analysis of all the catalyst samples

Catalyst sample	C (at%)	N (at%)	O (at%)	Surface area (m^2. g^{-1})	Pore size (nm)
N@C-g-C_3N_4-650	72.95	18.37	8.68	362	17.6
N@C-g-C_3N_4-750	79.34	13.43	7.22	570	19.7
N@C-g-C_3N_4 -850	86.05	6.68	7.28	870	15.7
N@C-g-C_3N_4-950	90.39	4.84	4.77	903	17.3
N@C-DCA-950	89.31	3.98	6.71	602	3.2
N@C-Mela-950	88.95	3.90	7.15	213	3.6
N@C-Urea-950	89.87	2.76	7.37	633	1.4

Table S2 The N species atomic ratio (calculation from XPS analysis) of all the catalyst samples

Catalyst sample	pyridinic N (%)	Pyrrodic N (%)	Graphitic N (%)	Oxidize N (%)
N@C-g-C_3N_4-650	31.15	18.16	2.61	48.08
N@C-g-C_3N_4-750	32.68	18.71	2.46	46.15
N@C-g-C_3N_4-850	14.87	28.83	28.15	28.15
N@C-g-C_3N_4-950	9.70	19.40	54.73	16.17
N@C-DCA-950	17.30	7.03	35.14	40.54
N@C-Mela-950	17.06	8.03	39.13	35.79
N@C-Urea-950	13.41	7.97	32.97	45.65